Journal of Information Display, vol. 5, no. 1, 2004 © 2004 KIDS

Dopant-Activation and Damage-Recovery of Ion-Shower-Doped Poly-Si through PH_3/H_2 after Furnace Annealing

Dong-Min Kim[a], Dae-Sup Kim[a], Jae-Sang Ro[a*], Kyu-Hwan Choi[b], and Ki-Yong Lee[b]

Abstract

Ion shower doping with a main ion source of P_2H_x using a source gas mixture of PH_3/H_2 was conducted on excimer-laser-annealed (ELA) poly-Si. The crystallinity of the as-implanted samples was measured using a UV-transmittance. The measured value of as-implanted damage was found to correlate well with the one calculated through/obtained from TRIM-code simulation. The sheet resistance was found to decrease as the acceleration voltage increased from 1 kV to 15 kV at a doping time of 1 min. However, it increases as the acceleration voltage increases under severe doping conditions. Uncured damage after furnace annealing is responsible for the rise in sheet resistance.

Keywords : LTPS (low temperature Poly-Si), ion shower doping, dopant activation

1. Introduction

Low Temperature Poly-Silicon (LTPS) technology is an important component in the fabrication of poly-Si TFT-LCD's and OLED's. Processing temperatures for the deposition of a-Si films, crystallization of a-Si into poly-Si, and dopant activation, are limited to below~600 ℃ due to glass substrate. Non-mass analyzed ion shower doping technique has been widely used for source/drain doping, for lightly doped drain (LDD) formation, and for channel doping in fabrication of low-temperature poly-Si thin-film transistors (LTPS-TFT's) [1-5]. Dopant activation may be done by furnace annealing, excimer laser annealing, and rapid thermal annealing, respectively [6]. Activation annealing is known to satisfy both the electrical activation of implanted impurities and the annealing of primary crystalline defects.

As the channel length is becoming shorter, device reliability of LTPS-TFT's must be taken into account [7, 8]. There are many factors that may affect the reliability of TFT devices, including the quality of poly-Si, the integrity of gate oxide, the degree of passivation of the interface between SiO_2 and Poly-Si, and damage near the triple junction of SiO_2/channel/ LDD. It is, therefore, important to wisely choose the energy and dose especially in the region of LDD. Here, damage recovery by activation annealing also plays an important role. It this study, we chose the wide range of ion energy and dose in order to understand the behavior of damage-generation and damage-recovery before and after activation annealing.

2. Experimental

The substrates used were poly-Si produced by excimer laser crystallization on 500 Å-thick PECVD (plasma enhanced chemical vapor deposition) a-Si. Phosphorous was implanted by ion shower doping with a main ion source of P_2H_x using a source gas mixture of PH_3/H_2 [9, 10]. Acceleration voltage was changed from 1 kV to 15 kV while doping time was varied from 10 sec to 3 min as variables of implantation conditions. Activation annealing was performed using a tube furnace in a nitrogen ambient. The sheet resistance was measured using a 4-point-probe. Crystallinity was determined by UV-transmittance and Raman spectroscopy, respectively. Surface roughness was measured using an atomic force microscopy.

Manuscript received October 6, 2003; accepted for publication April 8, 2004.
Corresponding Author : Jae-Sang Ro
* Members KIDS
a. Department of Materials Secience and Engineering, Hongik University, 72-1 Sangsu-dong, Mapo-ku, Seoul, 121-791, Korea.
b. Samsung SDI CO.,LTD.,Yongin -City, Gyeonggi-do, 449-902, Korea.
E-mail : jsang@hongik.ac.kr **Tel** : +2 320-1698 **Fax** : +2 334-0750

3. Results and Discussion

In order to observe the defect generation behavior for various doping conditions, we changed the acceleration voltage from 1 kV to 15 kV and the doping time from 1 min to 3 min, respectively. Fig. 1 shows the UV-transmittance as a function of wavelength for the as-implanted samples. Near the region of the wavelength between 350 nm and 550 nm, the transmittance spectrum shows sharp changed with the acceleration voltage. At a doping time of 1 min, we found that the acceleration voltage increased the slope at around 400 nm decreased, as shown in Fig. 1-(a). Then, the slope finally reached almost the value of a-Si at an acceleration voltage of 15 kV. As the doping time increased from 1 min to 3 min the change in the slope becomes greater, as indicated in Fig. 1-(b). These observations mean that the amount of damage, or, that of crystallinity, may correlate with the UV-slope at around 400 nm. We then differentiated the curves with regard to wavelength. Fig. 2 indicates the derivatives of Fig. 1 as a function of wavelength. We took the value of derivative at around 400 nm as the value of crystallinity. From Fig. 2, crystallinity, obtained from the value at 400 nm is seen to decrease as acceleration voltage increases. As the doping time increases from 1 min to 3 min, it decreases

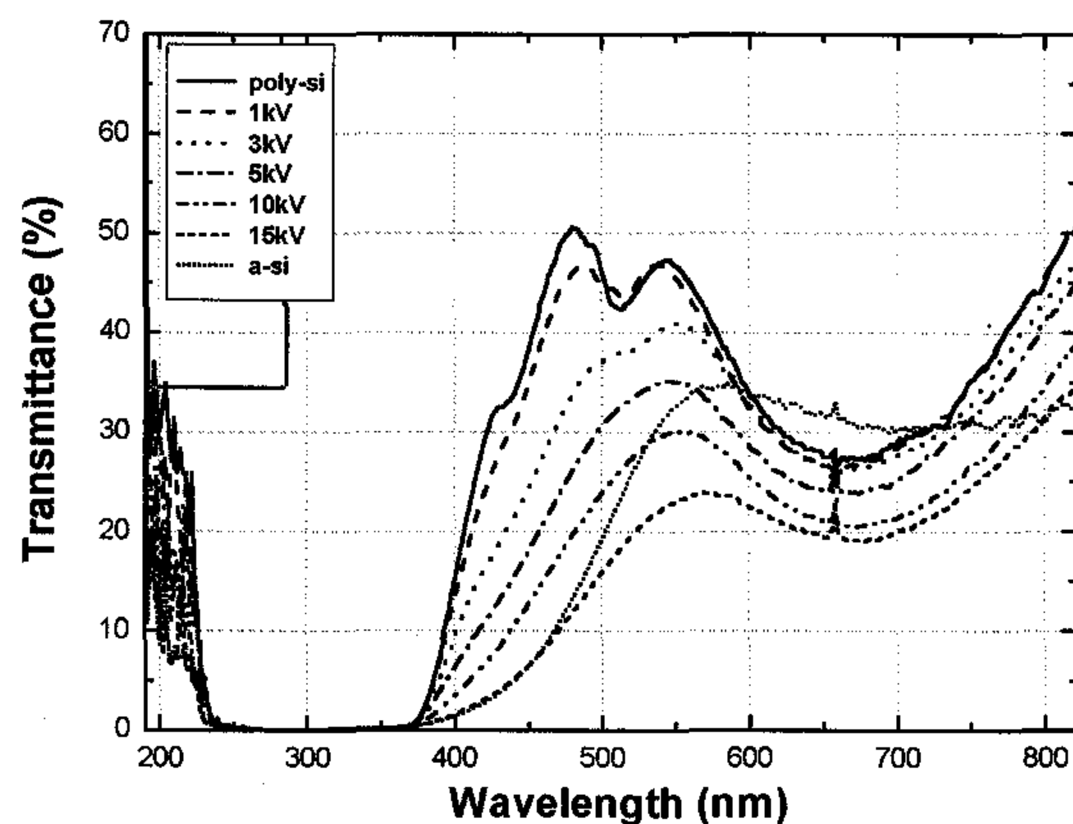

(a)

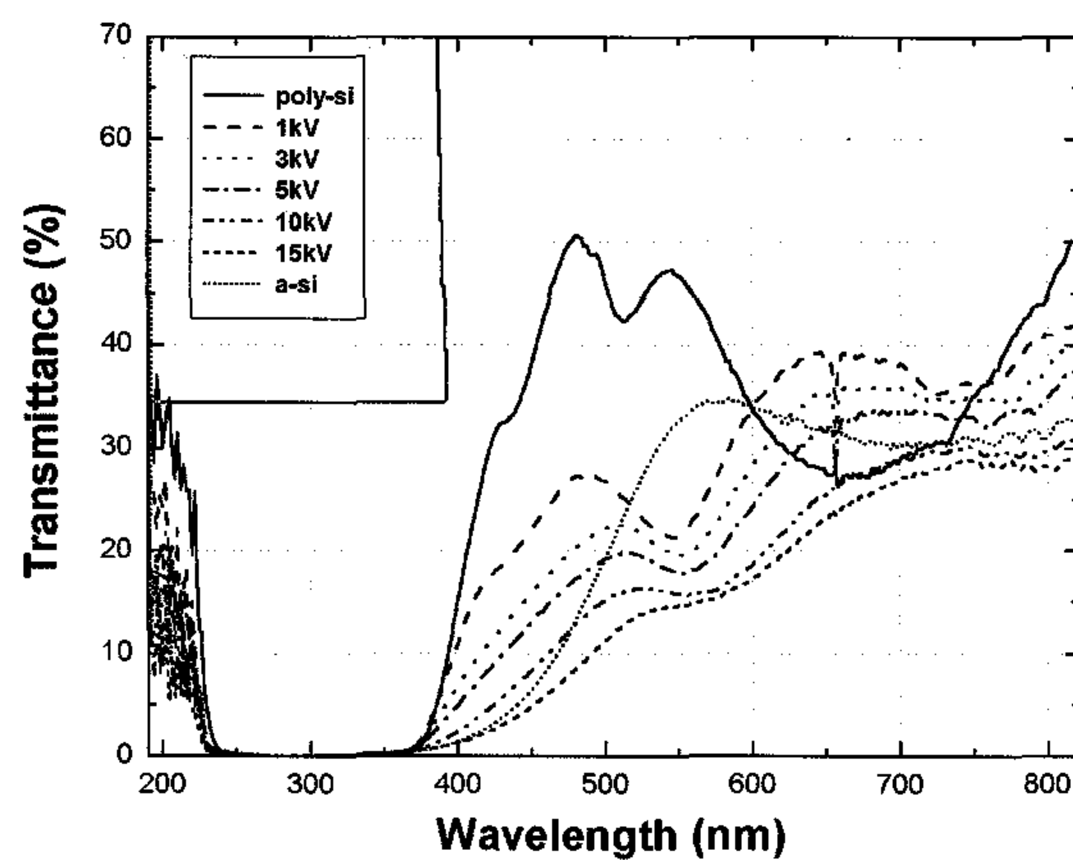

(b)

Fig. 1. UV-transmittance as a function of wavelength (a) for the as-implanted samples at a doping time of 1 min, and (b) for the as-implanted samples at a doping time of 3 min, respectively. The samples were implanted using acceleration voltages of 1, 3, 5, 10 and 15 kV, respectively. Note that the curves of ELA Poly-Si and a-Si are also indicated in the figures.

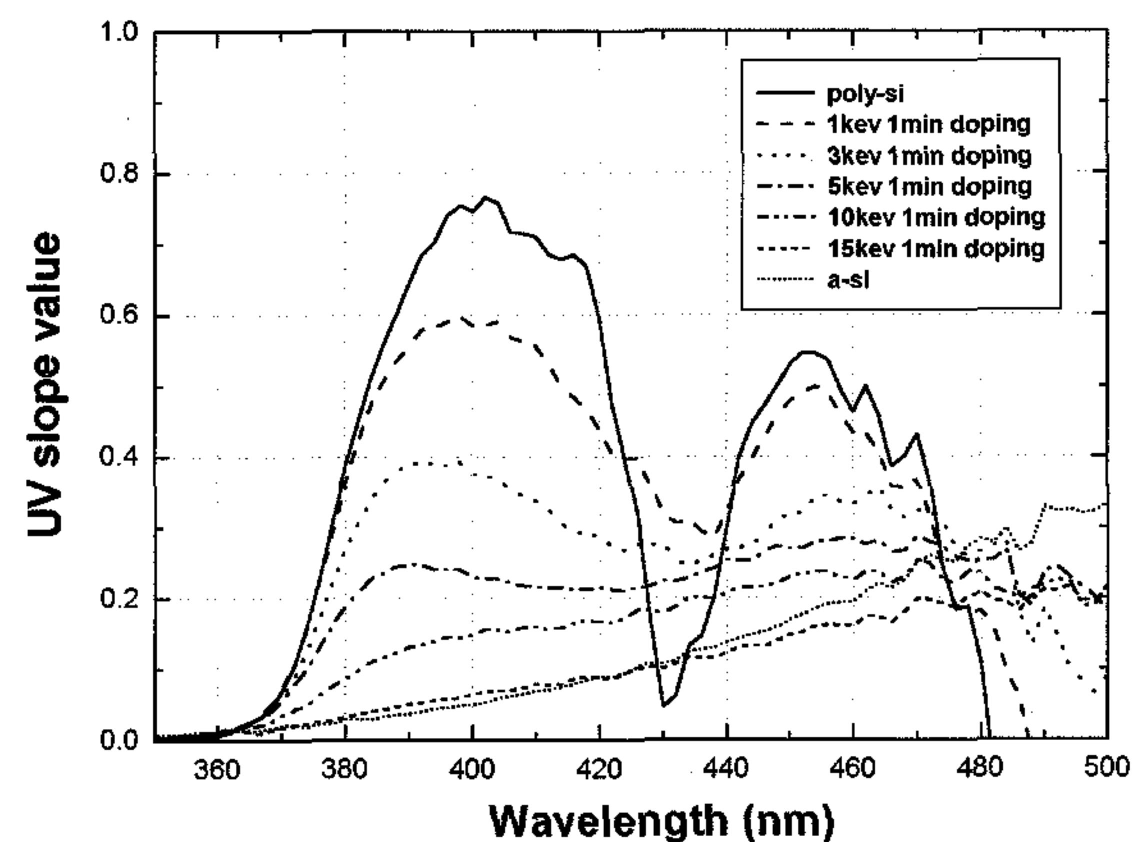

(a)

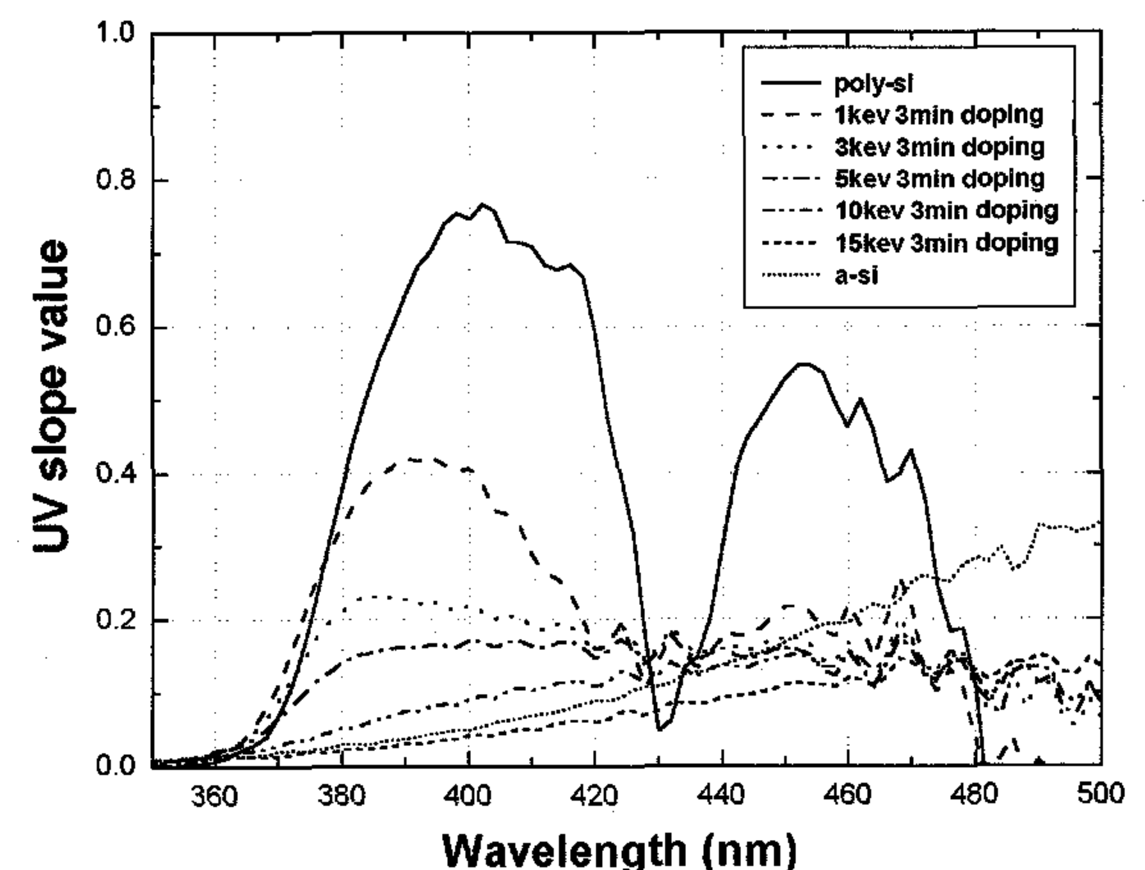

(b)

Fig. 2. Derivatives of Fig. 1 as a function of wavelength (a) for the as-implanted samples at a doping time of 1 min, and (b) for the as-implanted samples at a doping time of 3 min, respectively.

significantly as indicated in Fig. 2-(b). Fig. 3 shows the crystallinity obtained from Fig. 2 as a function of acceleration voltage for the samples doped at 1 min and 3 min, respectively. The values of crystallinity in Fig. 3 are normalized ones assuming that ELA poly-Si as a starting material has the value of 1.0. In order to check the validity of UV-transmittance method for determining the crystallinity, we conducted a Raman spectroscopy for the samples doped at 1 min. As indicated in Fig. 4, the UV-crystallinity has a strong correlation with the Raman-one. Fig. 5 shows the defect density calculated by TRIM-code simulation [8] as a function of acceleration voltage. The defect density was obtained by integrating a primary-defect concentration from 0 Å to 500 Å assuming a dose of $1\times10^{15}cm^2$. The amount of as-implanted damage induced in 500 Å-thick poly-Si films is seen to increase with the acceleration voltage. This trend is consistent with the results obtained by UV-transmittance as shown in Fig. 3. The measured crystallinity decreases with acceleration voltage and doping time. Crystallinity drops rapidly with the acceleration voltage within the range of 1 kV to 5 kV, and then mores gradually beyond 5 kV. The calculated defect density is seen to have a similar relationship with acceleration voltage

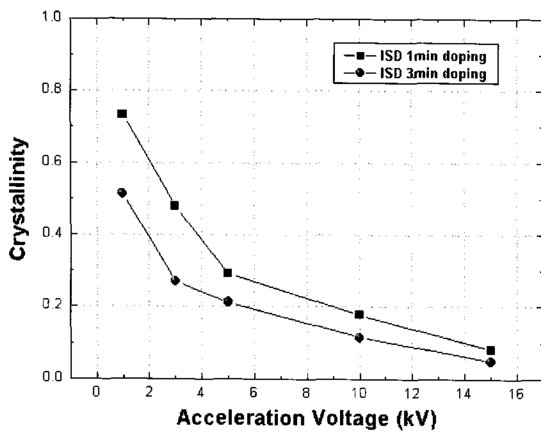

Fig. 3. Measured crystallinity vs. acceleration voltage using UV-transmittance for the samples implanted with 1 min and 3 min, respectively. The value of UV-slope at 400 nm was taken as crystallinity.

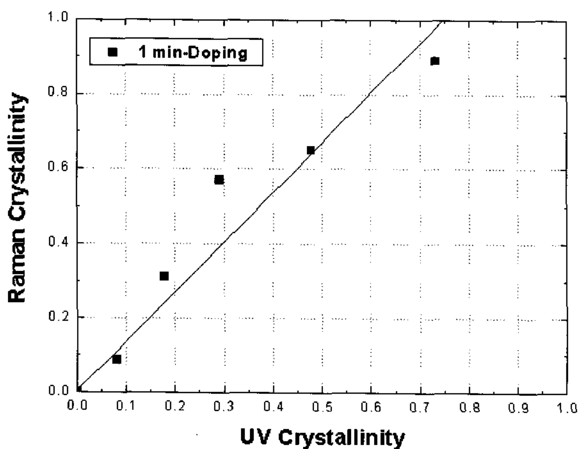

Fig. 4. Raman-crystallinity vs. UV-crystallinity. Note that they have a strong correlation .

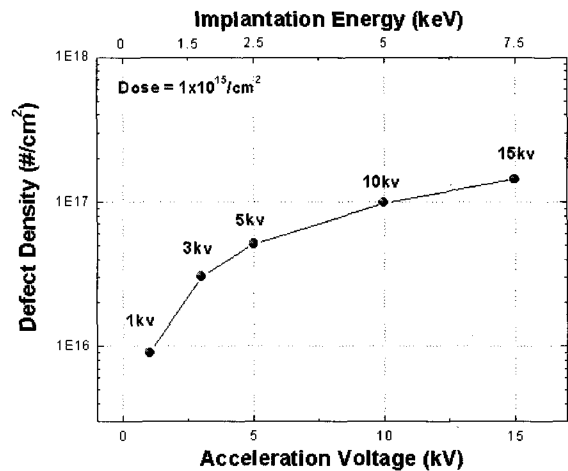

Fig. 5. Calculated defect density as a function of acceleration voltage using TRIM-code simulation. The defect density (#/cm^2) was calculated by integrating primary-damage profile from 0 to 500 Å.

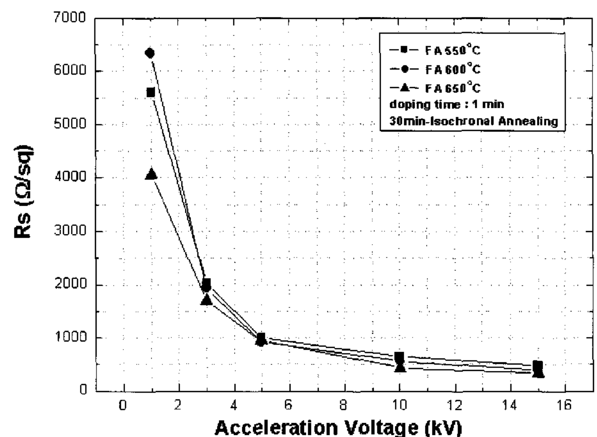

Fig. 6. Sheet resistance as a function of acceleration voltage. Annealing was conducted after ion shower doping at 550 °C (circles), 600 °C (squares), and 650 °C (triangles) for 30 min, respectively.

as implied in Fig. 5.

When we annealed the samples implanted at a doping time of 1 min within the range of 550 ℃ to 650 ℃ for 30 min, the sheet resistance was observed to decrease with the acceleration voltage as shown in Fig. 6. The sheet resistance was measured to be below the level of 1,000 Ω/□ for the samples implanted with acceleration voltages exceeding 5 kV regardless of the above annealing conditions. Fig. 7 shows the crystallinity for the as-implanted samples and for the annealed ones. As-implanted damage is recovered more and more as the annealing temperature increases from 550 ℃ to 650 ℃. Damage-recovery proceeds gradually with the annealing temperature and time, while the kinetics of dopant activation was found to be a relatively rapid process.

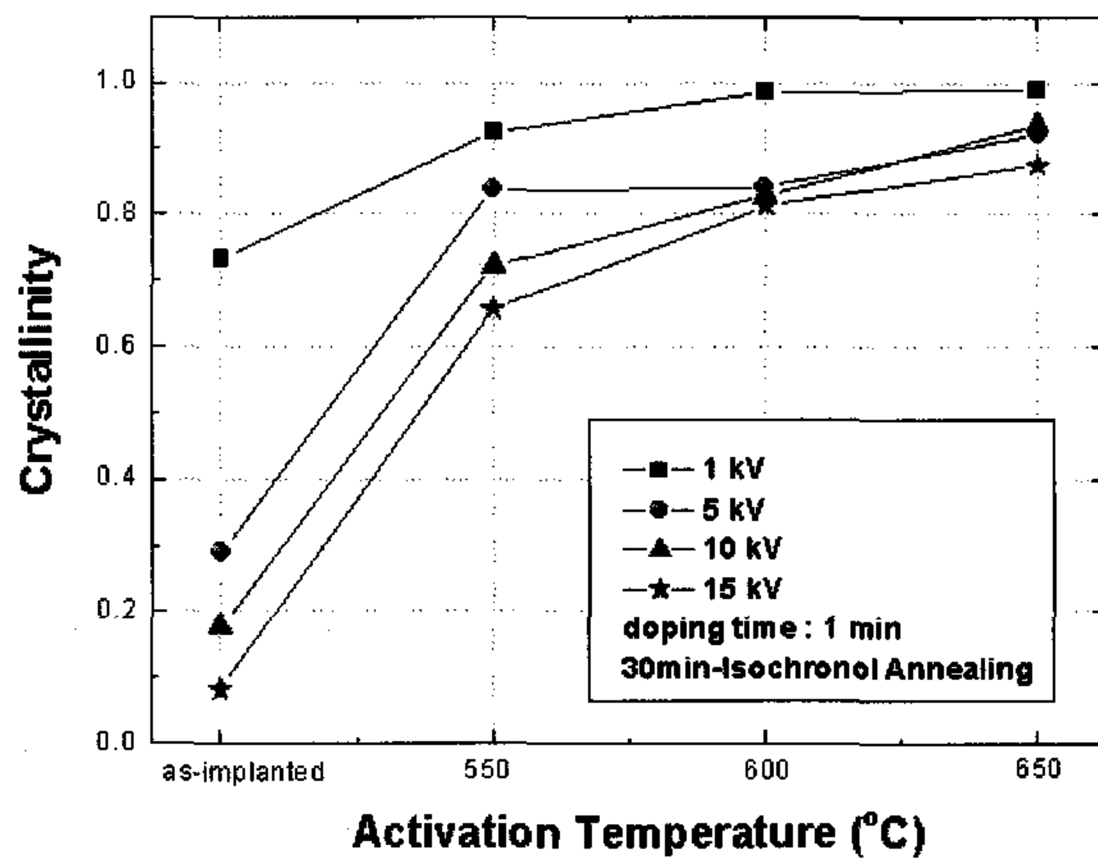

Fig. 7. Measured crystallinity for as-implanted samples and as-annealed samples, respectively.

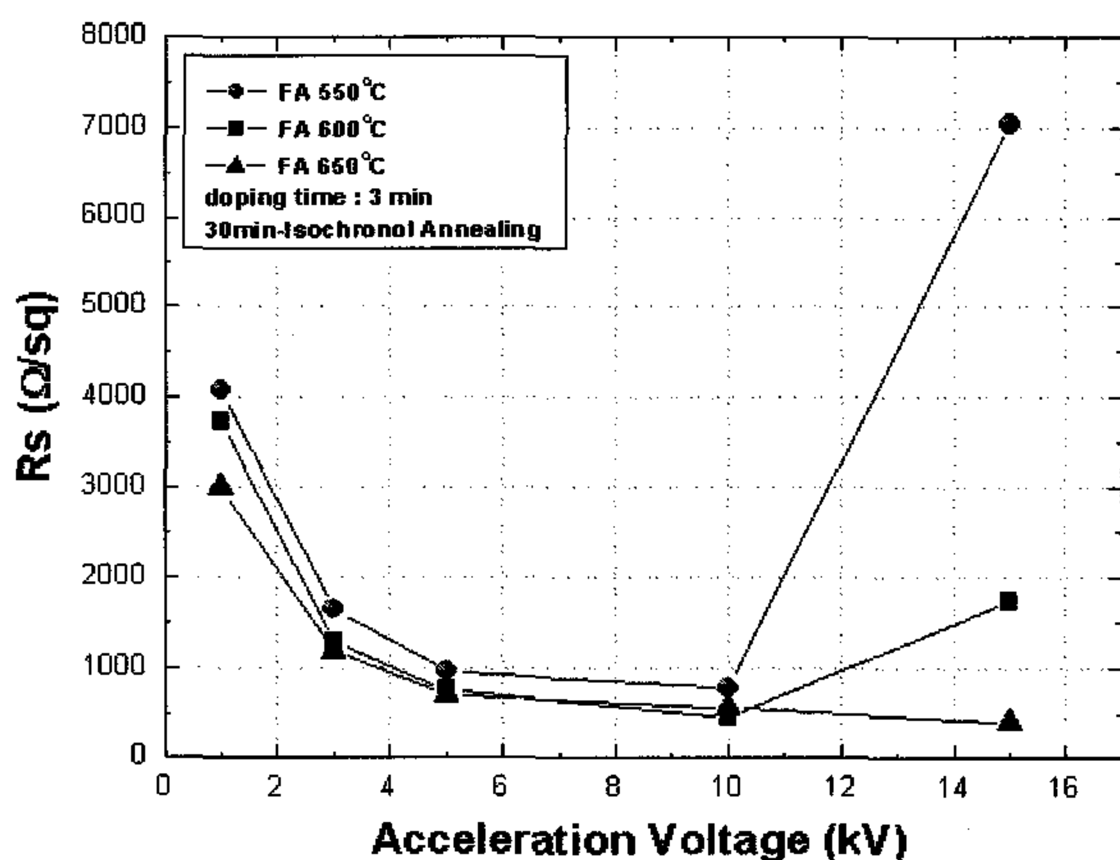

Fig. 8. Sheet resistance vs. acceleration voltage. The samples were annealed at 550 °C (triangles), 600 °C (circles), and 650 °C (squares) respectively after ion shower doping.

Fig. 8 shows the sheet resistance as a function of acceleration voltage for the samples implanted with a doping time of 3 min. The sheet resistance decreases with the increase in acceleration voltage within the range of 1 kV to 10 kV. However, it appears to increase for the 15 kV-implanted samples following a furnace annealing of within the range of 550 ℃ to 600 ℃ for 30 min, as indicated in Fig. 8. As shown in Fig. 9 damage was not yet recovered for these samples. This can be explained by the rise in sheet resistance. The sheet resistance does not, rise however, for the sample annealed at 650 ℃ for 30 min as demonstrated

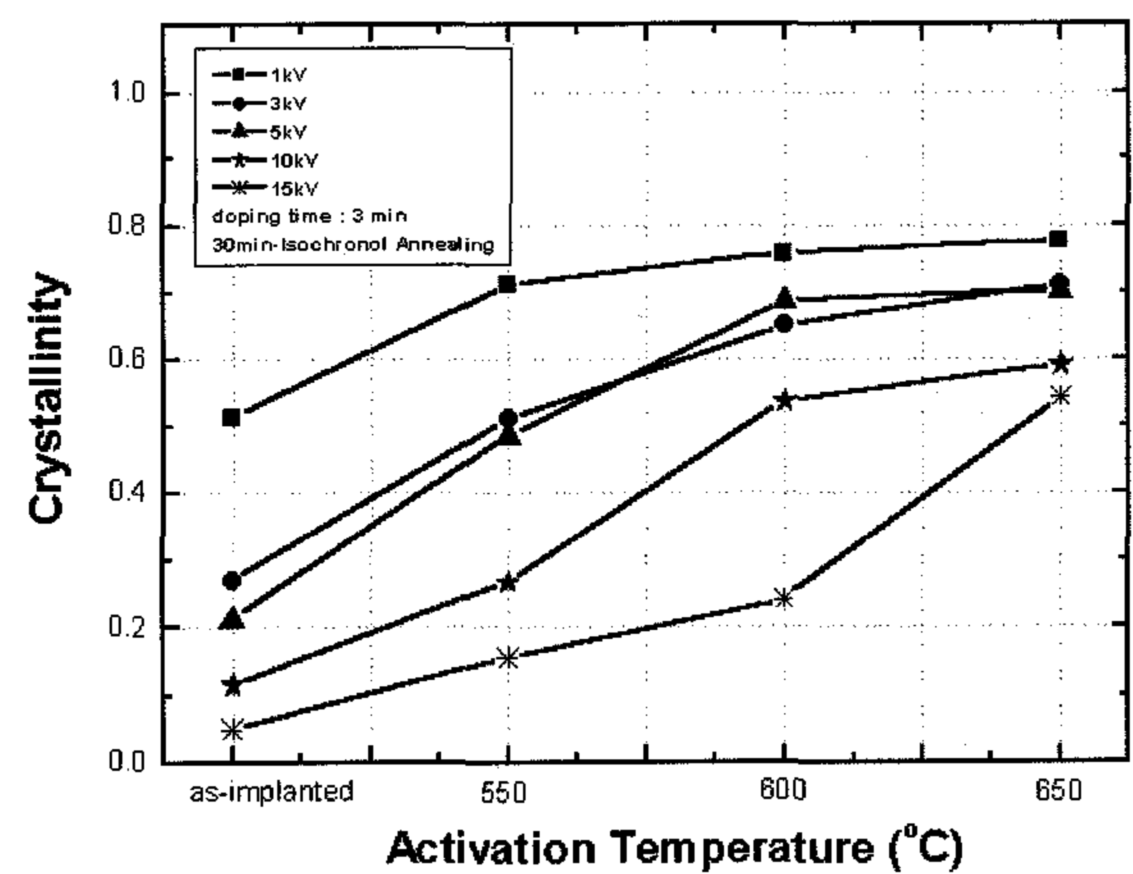

Fig. 9. Measured crystallinity for as-implanted samples and as-annealed samples, respectively. The samples were implanted at a doping time of 3 min with an acceleration voltage of 1, 3, 5 10, and 15 kV, respectively.

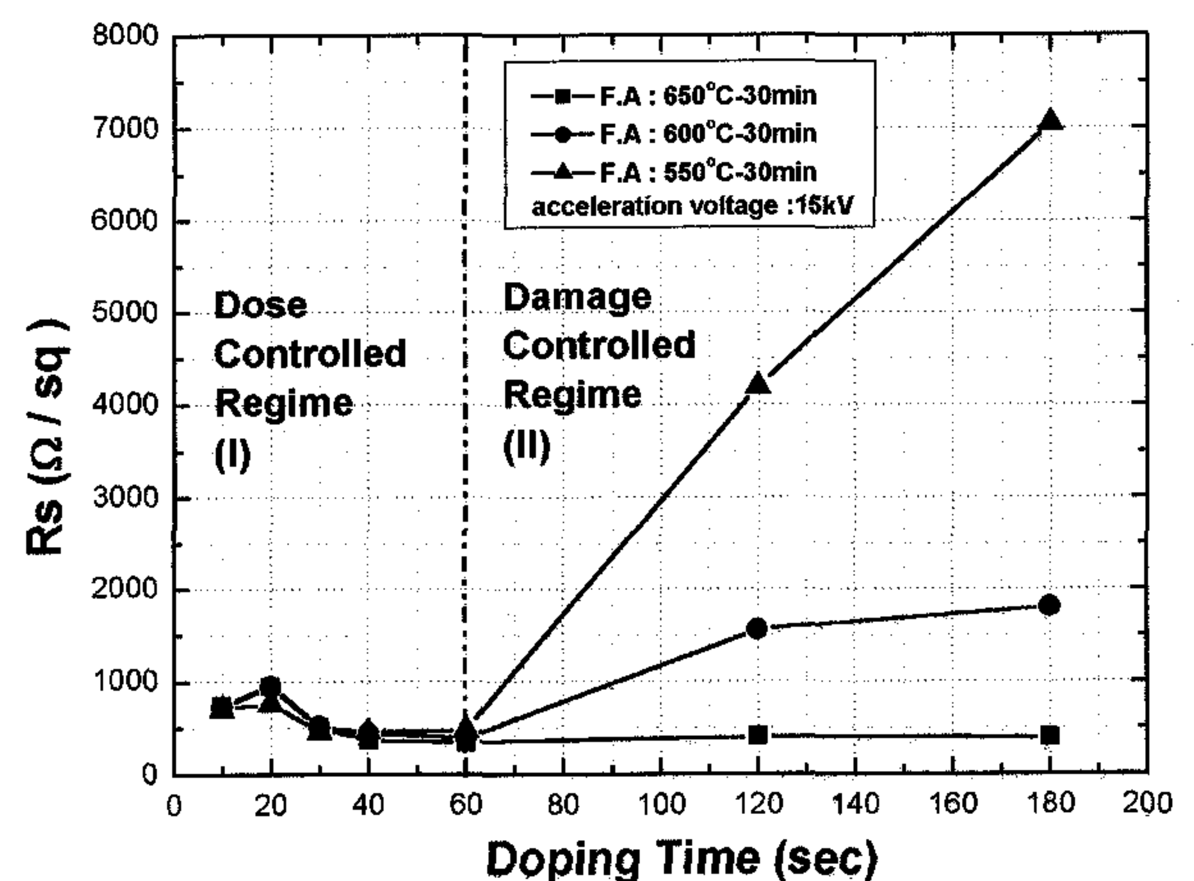

Fig. 10. Sheet resistance vs. doping time for the 15 kV-implanted samples annealed at 550 °C (triangles), 600 °C (circles), and 650 °C (squares), respectively.

in Fig. 8. In fact, the damage was recovered significantly for this sample as implied in Fig. 9.

Since the implantation condition with the acceleration voltage of 15 kV induces more damage than any other condition involved in this study we changed the doping time and annealing conditions by using the samples implanted with this voltage in order to investigate the characteristics of dopant activation and damage recovery. Fig. 10 shows the sheet resistance as a function of doping time of 30 min for the annealed samples at 550 ℃ (triangles), 600 ℃ (circles), and 650 ℃ (squares), respectively following ion shower doping of the acceleration voltage of 15 kV. The sheet resistance is seen to reache the value of below 1,000 Ω/□ within the doping time of 1 min. Furnace annealing for 30 min with the range of 550 ℃ to 650 ℃ showed almost the same efficiency level in terms of dopant activation within the doping time of 1 min. The sheet resistance also decreased and saturated within in this period of doping time, Regime I, Dose-Controlled-Regime as illustrated in Fig. 10. However, beyond the doping time of 1 min, the sheet resistance, increased except for the case of 650 ℃-30 min annealing. The rise in the sheet resistance resistance for the samples implanted at high dose was found to be the result of uncured damage as implied in Fig. 11. Cystallinity measured by UV-transmittance for the as-implanted samples at various doping time showed the value of below ~ 0.2. Crystallinity for the samples implanted for 2 min and 3 min was measured to be in the level of below ~ 0.3 even after annealing at 600 ℃, whereas that for 10 sec and 20 sec, the samples reached almost the value of ELA poly-Si. This observation clearly demonstrates that uncured damage is the cause of the rise of sheet resistance for the samples implanted with a heavy dose (Regime II : Damage-Controlled-Regime as illustrated in Fig. 10). Although the sheet resistance did not rise at a doping time beyond 2 min for the samples annealed at 650 ℃ for 30 min, the damage could not be sufficiently recovered as implied in Fig. 11.

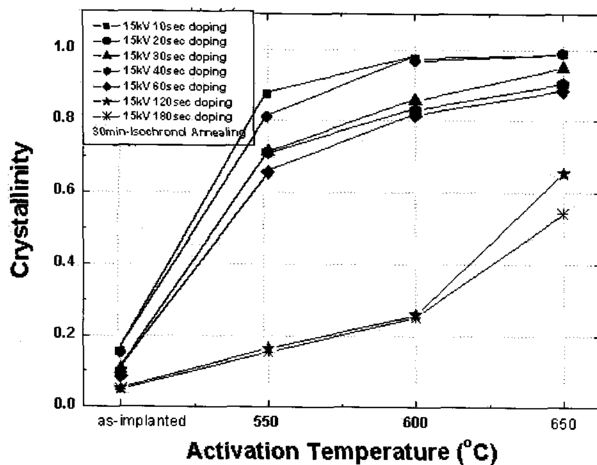

Fig. 11. Measured crystallinity for as-implanted samples and as-annealed samples, respectively. The samples were implanted at a doping time of 10, 20, 30, 40, 60, 120, and 180 sec with an acceleration voltage of 15 kV, respectively.

Fig. 12 and Table 1 show the surface roughness measured by an atomic force microscopy (AFM) for ELA-Poly, as-implanted and as-annealed Si, respectively. Implantation was conducted with 5 kV at a doping time of 3 min with a source gas of PH_3/H_2. Annealing was performed at 550 ℃ for 30 min after ion shower doping. The surface was found to become smooth after ion shower doping, presumably due to partial amorphization. Then, we observed that the it becomes rough again after annealing as damaged layer near the surface becomes recrystallized.

4. Conculsions

In summary, the UV-transmittance spectroscopy was demonstrated to be a good method for the crystallinity of the films. The measured UV-crystallinity showed to have a

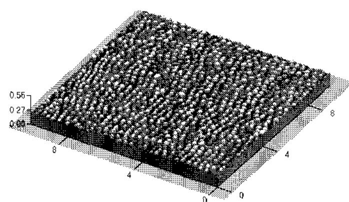

(a)

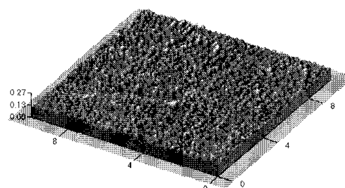

(b)

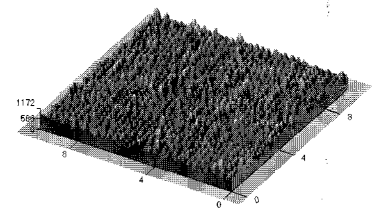

(c)

Fig. 12. AFM images for ELA Poly-Si, as-implanted Si, and as-annealed Si.

Table 1. Surface roughness for ELA-Poly, as-implanted, and as-annealed Si measured by AFM

Sample	Rms. roughness(Å)	Avg. roughness(Å)
ELA Poly-Si	176	144
as-implanted (5 kV-1 min)	144	114
as-annealed (550 ℃-30 min)	156	126

strong correlation with the measured Raman-crystallinity. The measured UV-crystallinity was also found to correlate well with the one calculated by TRIM-code simulation. Damage recovery was rather a slow process, whereas the kinetics of dopant activation was relatively rapid. Damage-recovery need to be taken into account in addition to dopant activation when choosing the most appropriates means of activation annealing. An annealing technique with sufficient thermal-budget is required for efficiently this curing damage.

References

[1] Y. Mishima and M. Takei, J. Appl. Phys. **75**, 4933 (1994).

[2] G. Kawachi, T. Aoyama, K. Miyato, Y. Ohno, A. Mimura, N. Komishi, and Y. Mochizuki, J. Electrochem. Soc. **137**, 3522 (1990).

[3] M. Yazaki, S. Takenaka, and H. Ohshima, Jpn. J. Appl. Phys., Part 1 **31**, 206 (1992).

[4] C. F. Yeh, T. Z. Yang, C. L. Chen, T. J. Chen, and Y. C. Yang, Jpn. J. Appl. Phys., Part 1 **32**, 4472 (1993).

[5] K. R. Olasupo and M. K. Hatalis, IEEE Trans. Electron Devices **8**, 1218 (1996).

[6] G. Kawachi, T. Aoyma, A. Mimura, and N. Konishi, Jpn. J. Appl. Phys. **33**, 2092 (1994).

[7] L. Mariucci, G. Fortunato, R. Carluccio, A. Pecora, S. Giovannini, F. massussi, L. Colalongo, and M. Valdinoci, J. Appl. Phys. **84**, 2341 (1998).

[8] D. -Z. Peng, T. -C. Chang, C. -Y. Chang, M. -L. Tsai, C. -H. Tu, and P. -T. Liu, J. Appl. Phys. **93**, 1926 (2003).

[9] K. Chen, G. J. Ra, Y. Shao, G. Mo, S. Lichtenthal, and J. Blake, *Proc. of 1998 International Conference on Ion Implantation Technology*. (1998), p. 1218.

[10] Y. -S. Kim, Master Thesis, Hongik Univeristy (2000).

[11] J. F. Ziegler, J. P. Biersack, and U. Littmark, in *The stopping and Range of Ions in Solids, Vol. 1 of The Stopping and Range of ions in Matter*, ed. by J. F. Ziegler (Pergamon, New York, 1985), p. 25.